Wear 266 (2009) 1165–1170

Contents lists available at ScienceDirect

Wear

journal homepage: www.elsevier.com/locate/wear

Frictional and adhesive behavior of organic–inorganic hybrid coatings on surgical grade stainless steel using nano-scratching technique

Josefina Ballarre[a,b,*], Damián A. López[b], Ana L. Cavalieri[a]

[a] Structural Materials Lab. – Ceramics Division, Material's Science and Technology Research Institute (INTEMA), UNMdP-CONICET, Juan B. Justo 4302, B7608FDQ Mar del Plata, Argentina
[b] Corrosion Division, Material's Science and Technology Research Institute (INTEMA), UNMdP-CONICET, Juan B. Justo 4302, B7608FDQ Mar del Plata, Argentina

ARTICLE INFO

Article history:
Received 23 August 2007
Received in revised form 18 February 2009
Accepted 23 March 2009
Available online 2 April 2009

Keywords:
Hybrid coating
Sol–gel
Nano-scratch test
Adhesion
Friction coefficient

ABSTRACT

Because of their mechanical properties, metals are the most widely used materials as orthopaedic implants. However they cannot provide a natural bond with the mineralized bone and they also release metallic particles due to degradation or tribologic events. One way to improve the metallic implants performance is to apply protective organic–inorganic sol–gel coatings. In this work, stainless steel substrates are coated with films made by a sol–gel technique from organosilane precursors.

Although mechanical properties of similar films have been studied, there is no information about adhesion, friction or deformation processes of silica-based hybrid films to stainless steel substrates.

Hybrid coatings with higher amount of inorganic components (called TMH) have almost no elastic response and the debris due to chipping or delamination does not persist into the indentation trace. With the film with high content of organic compounds was found elastic recovery in early stages of loading and there is evidence of pile-up at the edges of the trace with higher load applied. After the unloading the film has a persistent deformation and is removed due to the asynchronic recovery of the film and the substrate. The combined two-film coating shows a lot of debris in the trace. This is an unusual but possible behavior of polymeric coatings and could be attributed to different recoveries between the first inorganic layer (called TEOS–MTES), the substrate and the upper TMH film. This fact produces delamination and crack formation in the TEOS–MTES coating, inducing tensile efforts, and finally the upper film is pulled-off.

1. Introduction

A lot of biomaterials are used in medicine, but not all of them can be used for orthopaedic purposes because of the high mechanical properties required. The most widely used materials are inert metals [1]. However, there are problems when is necessary to create a natural union with the mineralized bone and these materials could release metallic particles to the surrounding media. This fact can cause different pathologies that could finally lead to the removal of the implant [2,3]. One way to improve the metallic implant performance consists in the application of protective films [4,5]. These coatings are mainly made from alcoxide precursors of SiO_2 that create vitreous and uniform films. These films can be functionalized introducing particles in the system, or can be bioactive themselves [6–10].

A disadvantage of glassy coatings is their brittleness. The hybrid organic–inorganic films with high content of silica are presented as an alternative to improve the mechanical properties of vitreous coatings preserving an interesting property of them: to be a protective and dense net [11,12]. In addition, the incorporation of hydroxides with some organic groups is expected to give plastic characteristics to the films. In order to make thicker films, coatings with high proportion of organic compounds have been recently obtained. These films are able to contain bioactive particles that are not easily released to the media [13].

These thin films provide the material the capability to be a bio-inert connector between the metallic prosthesis and the bone tissue. Also, superficial features as the roughness or friction coefficient and the adhesion of the coating to the substrate are of great importance for a complete mechanical characterization. Usually, the orthopaedic doctors do not pay special attention in the type of material or if it is a coated one at the time the implant is been inserted in the body. The implanting procedure is performed by applying high tension and loads on the metal. Because of this, it is important to know the mechanical, adhesive and wear properties and behavior of the implant surface in order to avoid future failure of

* Corresponding author at: Juan B. Justo 4302, B7608FDQ Mar del Plata, Argentina. Tel.: +54 223 481 6600; fax: +54 223 481 0046.
E-mail address: jballarre@fi.mdp.edu.ar (J. Ballarre).

0043-1648/$ – see front matter © 2009 Elsevier B.V. All rights reserved.
doi:10.1016/j.wear.2009.03.029

the prosthesis. There is no information about the friction coefficient or the adhesion of silica-based hybrid organic inorganic coatings on stainless steel although their Young's modulus and hardness were recently analyzed [14] and mechanical properties of similar films have been studied [15–17].

One of the most recent techniques used to study the mechanical properties of thin films is the instrumented indentation, known as nanoindentation. This is a superficial technique to measure quasi-statically the penetration of an indenter at increasing loads applied to a material. With a modulus of lateral force, and a ramped load in a displacement (scratch) path, the nano-scratching test is implemented [18–22].

The aim of this work is to advance in the knowledge of the frictional and adhesive behavior of organic–inorganic hybrid silica-based thin coatings deposited on stainless steel used in orthopaedic surgery, employing the nano-scratching technique.

2. Experimental procedure

Flat samples of stainless steel AISI 316L were used as substrates. Before the application of coatings, they were successively cleaned in a soap solution and isopropylic alcohol in an ultrasound bath for 5 min. Finally, they were rinsed with distilled water and dried with hot air.

Two types of sols were used to make different coatings: TEOS–MTES and TMH (composed by TEOS–γMPS–HEMA). The starting materials were TEOS = tetraethoxysilane (ABCR); MTES = methyltriethoxysilane (ABCR); γMPS = 3-methacrylopropyl trimethoxysilane (Dow Corning) and HEMA = 2-hydroxyethyl methacrylate (Aldrich).

The TEOS–MTES sol was prepared by acid catalysis method in one stage, using TEOS and MTES as silica precursors; absolute ethanol as solvent and 0.1N nitric and acetic acids as catalysts. Water was incorporated from the nitric acid solution in stoichiometric ratio. The molar ratio of TEOS/MTES was 40:60. All the reagents were stirred at 40 °C for 3 h obtaining a transparent sol (pH 1–2, viscosity = 2.6 mPa s). The TMH sol was made in a two-step procedure using 0.1N nitric acid and isopropylic alcohol. The solution, containing 40 g l^{-1} of SiO_2, was stirred at 65 °C for 36 h in a glycerine bath.

Coatings were obtained by dip-coating at room temperature and withdrawn at 25 cm min^{-1}. Three different types of coatings were applied on the stainless steel substrates:

(a) Single coating consisting for one layer of TEOS–MTES sol treated at 450 °C for 30 min in air.
(b) Single coating (double-layer) consisting for two layers of TMH sol applied successively. The first layer was air dried for 30 min at room temperature, and the second layer was air treated for 60 min at 150 °C.
(c) Double coating consisting for a first layer of the TEOS–MTES hybrid, air treated at 450 °C for 30 min (type a), followed by a second double-layer of TMH (type b) coating, air treated for 60 min at 150 °C.

Immediately after film deposition on a glass substrate, a scratch was made with the aim of measuring coating thickness by using a profilometer (Talystep, Taylor-Hobson, UK). The final value was calculated as the average of three measurements.

The nano-scratch tests were performed using a nano-indenter XP, MTS NanoInstruments [23] (force resolution: 50 nN; displacement resolution: 0.1 nm) equipped with a nano-scratch attachment that allows lateral force measurements. A pyramidal diamond Berkovich indenter (tip radius = 1 μm) was used to produce the wear of each coating/substrate system and a 1400 μm scratching track was applied in all tests. The experimental procedure is shown in Fig. 1. At first (pre-scan step), the tip approaches the surface under default conditions, and then the load is maintained (0.1 mN) through all the scratch distances (200 μm initial + 1000 μm straightforward scratch + 200 μm final). An initial surface profile of the samples is made before scratching. In the second step (scratching), the tip starts to scratch at 200 μm from the start of the experiment with a ramped load to the distance of 1200 μm (final maximum applied load of 300 mN), where the load is removed to the initial one (0.1 mN) and maintained constant for 200 μm more. The surface profile could be sensed by the depth-sensing system. In the third step (post-scan) the test is done as was described in the pre-scan to measure the elastic recovery after scratching.

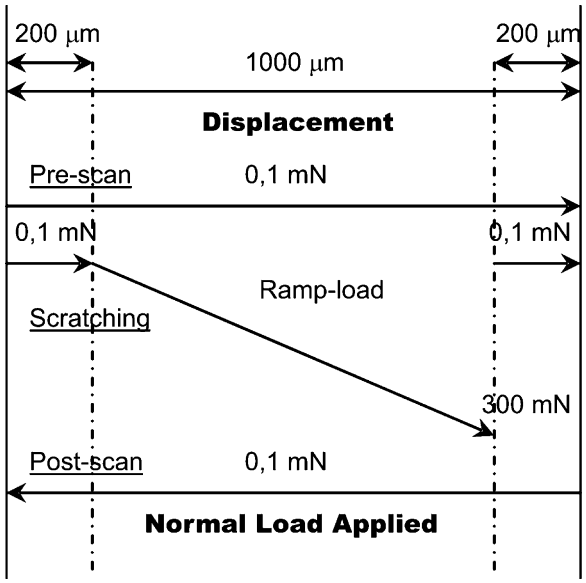

Fig. 1. Schematic diagram of the different steps for the experimental scratch test procedure.

Lateral (friction) forces are calculated from the stiffness measured in the calibration tests using fused silica as model material. The coefficient of friction is calculated by taking the ratio of the lateral force and the normal load applied on the indenter [22].

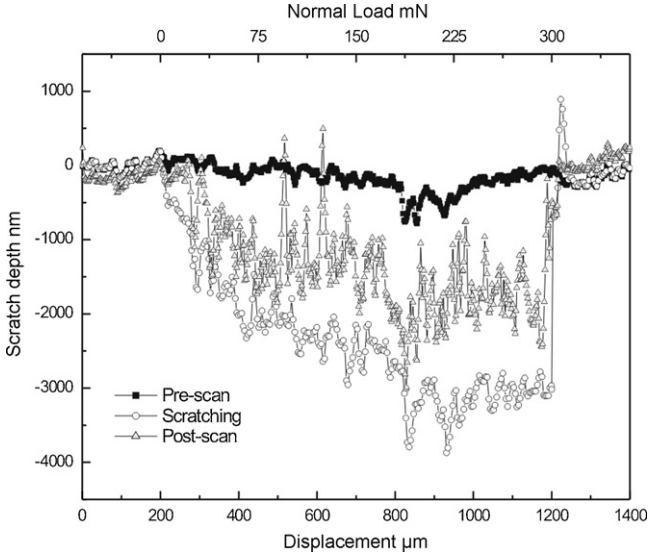

Fig. 2. Scratch depth profile versus normal applied load and horizontal displacement of the indenter tip on the TEOS–MTES coating on surgical grade stainless steel. The pre-scan, scan and post-scan made are shown.

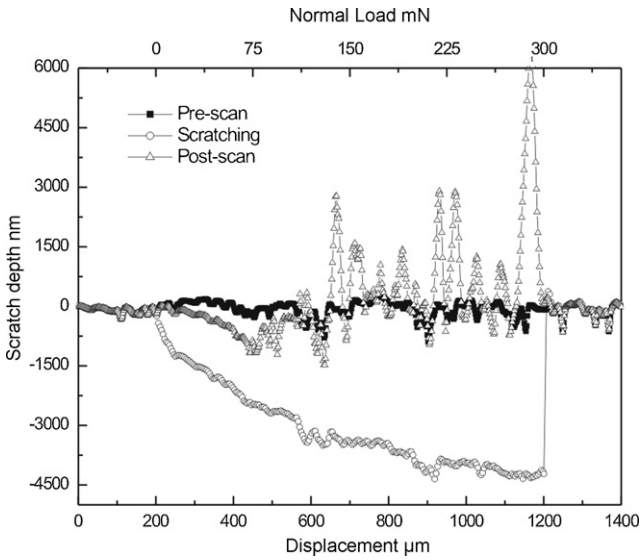

Fig. 3. Scratch depth profile versus normal applied load and horizontal displacement of the indenter tip on the TMH coating on surgical grade stainless steel. The pre-scan, scan and post-scan made are shown.

In a previous work of the authors [14], the Young's modulus and hardness of the types of coatings studied here were determined using a nanoindentation technique. The yield under load (creep) was also studied.

3. Results and discussion

The average thickness measured for each type of coating: TEOS–MTES, TMH and TEOS–MTES/TMH films were 1.2, 3.5 and 3.8 μm, respectively.

The adhesive behavior of the three types of films was analyzed with the results of the nano-scratch tests, looking for delamination, plowing or deformation events.

Figs. 2–4 show the surface profiles of stainless steel plates with TEOS–MTES, TMH and the dual TEOS–MTES/TMH coatings, respectively. The scratch depths (nm) are plotted as a function of both the horizontal displacements (μm) and the normal load applied (mN). The curves illustrate the sample behavior during the pre-scan, scratching and post-scan test steps. The initial scan at a continuous low load applied is used to analyze the roughness of the film surface through the pre-scan profile obtained. This profile in relation to the post-scan one is used to evaluate surface damage, debris production and elastic–plastic deformation after the scratching. Negative depths correspond to the scratch indenter being pushed into the film, and positive depths indicate outward blistering of the surface or the accumulation of debris during the scratch test.

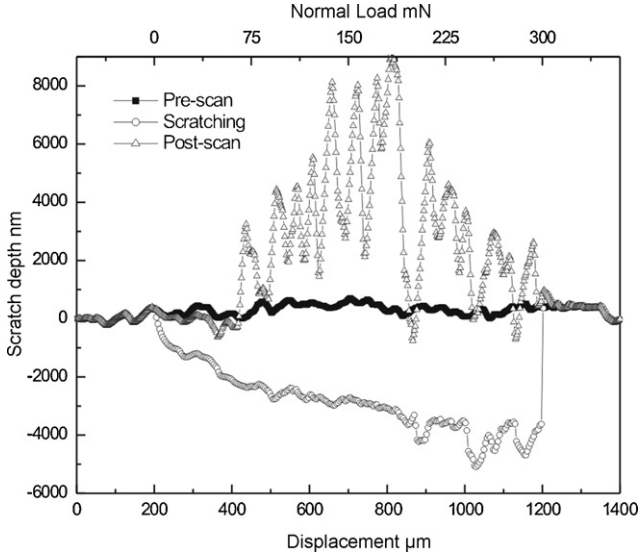

Fig. 4. Scratch depth profile versus normal applied load and horizontal displacement of the indenter tip on the TEOS–MTES/TMH coating on surgical grade stainless steel. The pre-scan, scan and post-scan made are shown.

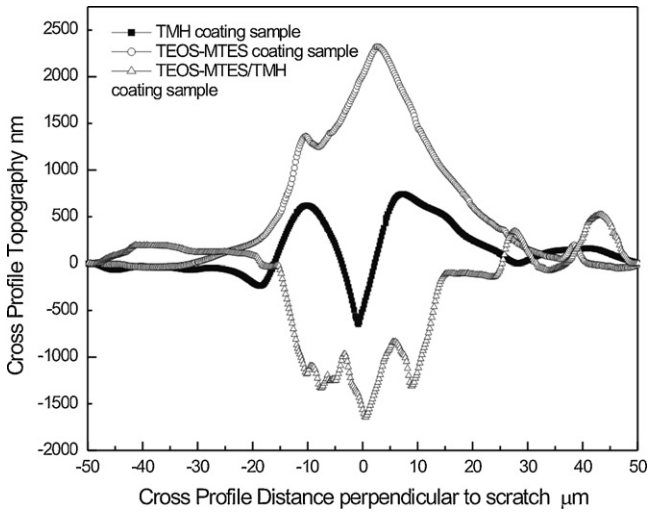

Fig. 5. Cross-profile topography as a function of cross-profile distance, perpendicular to scratch of the three types of coatings: TEOS–MTES, TMH and TEOS–MTES/TMH on surgical grade stainless steel.

In Fig. 2 can be observed the scratch distance versus the applied normal load (or the horizontal displacement) of the coating with the largest proportion of inorganic compounds (TEOS–MTES). In this case, it can be observed that the normal load applied is not proportionally linear with the penetration depth. This event could be attributed to some elastic recovery due to the amount of organic compounds present in this coating.

In the ramped load step (or scratching trace), a fluctuation in the register can be seen almost from the beginning of the load increment. This fact could be due to the presence of chipping, a type of delamination. Chipping is produced by radial crack formation

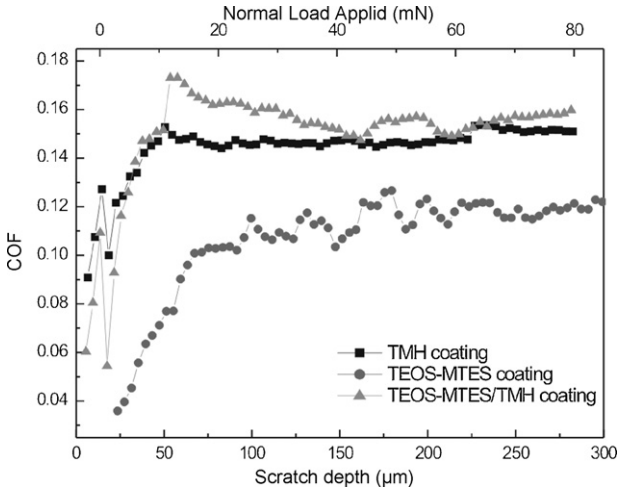

Fig. 6. Coefficient of friction (COF) as a function of increasing normal load and scratch distance of the three types of coatings: TEOS–MTES, TMH and TEOS–MTES/TMH on surgical grade stainless steel.

and delamination, and the area of damage is delimitated by the radial cracks [24]. During the post-scan step a residual damage in the material can be observed. The depth values do not recover to the initial values registered in the first step of the test, and hence, there is a permanent plastic deformation which can be inferred a peel-off of the film, with the deposition of some debris in the indenter trace. As with soft materials, no significant plowing was observed. He agrees with the fact that the coating is the one with the higher inorganic character (TEOS–MTES). There is evidence of removed material from the beginning of the test which was pushed ahead by the top of the tip and piled up at the sides of the trace. This transference of material can be confirmed in the cross-section topography (Fig. 5).

Fig. 3 shows for TMH coating a non-linear behavior of the normal load applied as a function of the penetration depth at the beginning of the scratch displacement (about 50 μm). After this distance, the increment in the normal load is proportional to the penetration until about 450 μm (applied normal load: 75 mN). This value is higher than the coating thickness and the indenter reaches the substrate. During the post-scan step, a complete elastic recovery of the film in the initial 100 μm of displacement and a small plastic deformation up to 450 μm (75 mN) can be observed. At this load the graph shows a discontinuity, corresponding to deformation mechanisms and pile-up in the edges of the trace. During the scratching step, a plastic deformation takes place with the increment of the load because of the organic characteristics of the film which does not delaminate. After the unloading, the films show delamination due to an asynchronic recovery of the film and the substrate. The positive values of penetration depth observed in Fig. 3 could be related to debris production or released particles by fracture or

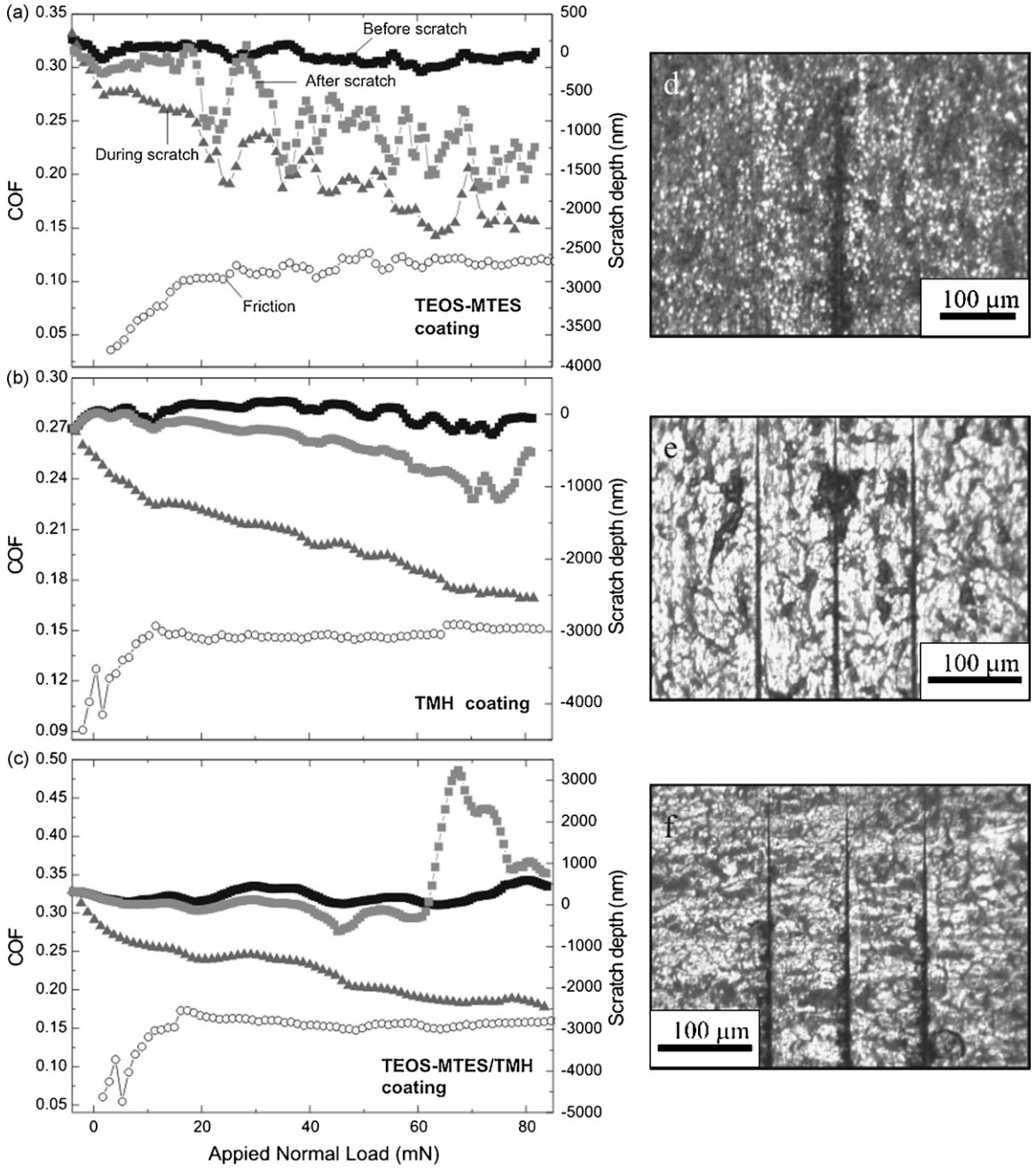

Fig. 7. Coefficient of friction (COF) and scratch depth profiles as a function of increasing normal load (a–c) and optical images (d–f) of the TEOS–MTES, TMH and TEOS–MTES/TMH coatings on surgical grade stainless steel after nano-scratch experiment. The optical images were taken at the beginning of the scratch process.

deformation events that have fallen into the trace. The cross-section of the scratch (Fig. 5) shows the traditional shape with a sharp deep "V" style when pile-up is the dominant event, typically found in polymeric materials [25]. So, it s inferred that the material has been moved to the sides (pile-up) of the trace on the TMH coating.

Fig. 4 shows the results of the scratch test on the dual TEOS–MTES/TMH coatings. Up to a 200 μm displacement under applied ramped load, it could be seen in the post-scan step that the recovery of the coating is almost complete (elastic behavior). This fact is attributed to low penetrations (due to the low loads applied) that do not reach the substrate or lead to any effect of the substrate on the film. At higher applied loads, there are no significant fluctuations in the scratching curve, until a depth penetration of 4 μm is reached, corresponding to the film thickness.

When the applied normal load is higher than 75 mN, positive values in the penetration depth can be seen in the post-scan of the dual coated material. This fact is due to released particles of the film that are introduced to the trace, an unusual but possible behavior in polymeric coatings [25]. The high quantity of removed material present in the scratch trace could be attributed to an asynchronic or different recoveries of the system substrate/TEOS–MTES hybrid (type a)/TMH coating (type b). This mismatch produces delamination and crack formation in the TEOS–MTES coating inducing tensile tensions, and finally leading to the fact that the upper film is pulled-off. In the cross-section topography (Fig. 5) the shape observed can be attributed to the removed material displaced onto the centre of the trace.

In Fig. 6, the coefficient of friction (COF) of the three types of coatings studied is plotted as a Function of the normal load applied and the displacement. For all coatings, there is an initial range (between 0 and 100 μm) where can be noticed an abrupt increment in the friction coefficient. This effect could be attributed to the different penetration depths of the indenter tip into the different types of coatings, removing in each case different quantities of materials by plowing or peel-off.

The most inorganic coating (TEOS–MTES) denoted the lowest friction coefficient ($COF_{TEOS-MTES} \sim 0.12$). The organic TMH and the dual TEOS–MTES/TMH coatings have similar values of coefficient of friction ($COF_{TMH} \sim 0.15$ and $COF_{TEOS-MTES/TMH} \sim 0.16$, respectively). The last two types of coatings have almost the same COF until the applied load reaches 60 mN: the penetration onto the film is the same which is attributed to the same upper coating of TMH in both cases. The abrupt change in the COF of the dual coating film can be associated to a secondary effect of the chipping occurring in the inner TEOS–MTES coating. After this applied load, the fluctuations in the COF value are similar to that found for the TEOS–MTES film.

A more detailed analysis is made by comparing the beginning (up to applied normal load = 80 mN) of the pre-scan, scratching and post-scan curves with the COF curves (Fig. 7a, b, and c for TEOS–MTES, TMH and TEOS–MTES/TMH, respectively). The optical images of the three coatings are also shown (Fig. 7d–f). For the TEOS–MTES coating, it can be certainly pointed that the film remains with a constant elasto-plastic deformation until 20 mN. At higher loads the tip of the indenter reaches the substrate (film thickness = 1.2 μm) and the failure of the coating by delamination is observed. Some fluctuations are observed in the COF after 25 mN because of the release of debris caused by the chipping process.

In the case of the TMH and the TEOS–MTES/TMH coatings, the thickness of the films (3.5 and 3.8 μm, respectively) are higher than the thickness of coating with only TEOS–MTES, and the substrate is not reached in the range of loads analyzed. The initial behavior is similar in both materials, until a load of 15 mN. Elastic deformation is observed and it is associated with the indenter penetration in the coatings at low loads, as can be seen in the COF curve (Fig. 7b and c). The deformation continues in both cases, but there is a change in the TEOS–MTES/TMH system behavior, associated to the fracture of the inner and more inorganic coatings (TEOS–MTES). The chipping of the coating that is caused by the formation of radial cracks is observed optically in the photograph beside the TEOS–MTES/TMH scratch curve (Fig. 7f).

4. Conclusions

The nano-scratch technique was successfully used for mechanical characterization of hybrid organic–inorganic thin films. The adhesive behavior of the three types of films was analyzed in order to distinguish deformation events, delamination or plowing.

1. The film with highest inorganic content (TEOS–MTES) has almost no elastic response but their debris or the material removed due to chipping or delamination does not persist into the indentation trace.
2. The film with high content of organic compounds (TMH) has elastic recovery until 75 mN of applied load. The coating suffers plastic deformation but not delamination. After the unloading, the film has a persistent deformation and is removed due to the asynchronic recovery of the film and the substrate.
3. The TEOS–MTES/TMH coating shows a lot of debris in the trace. This is an unusual but possible behavior and could be attributed to different recoveries between the substrate, the first TEOS–MTES layer and the upper TMH film. This fact produces delamination and crack formation in the TEOS–MTES coating, inducing tensile tensions, and finally the upper film is pulled-off.
4. The film with highest inorganic content (TEOS–MTES) denotes the lowest friction coefficient. The TMH and the dual TEOS–MTES/TMH coatings have similar values, indicating that the lower inorganic layer does not affect the friction with low loads applied.

Acknowledgments

The authors would like to thank Mark Anglada, Emilio Jimenez and Yves Gaillard from the Universitat Politécnica de Catalunya for their help with the indentation samples. The help of Dr. Florencia Sangermano is gratefully acknowledged.

References

[1] J.V. Sloten, L. Labey, R.V. Audekercke, G. Van der Perre, Materials selection and design for orthopaedic implants with improved long-term performance, Biomaterials 19 (16) (1998) 1455–1459.
[2] Y. Okazaki, E. Gotoh, T. Manabe, K. Kobayashi, Comparison of metal concentrations in rat tibia tissues with various metallic implants, Biomaterials 25 (28) (2004) 5913–5920.
[3] T. Hanawa, S. Hiromoto, K. Asami, Characterization of the surface oxide film of a Co–Cr–Mo alloy after being located in quasi-biological environments using XPS, Appl. Surf. Sci. 183 (1–2) (2001) 68–75.
[4] J. de Damborenea, N. Pellegri, O. de Sanctis, A. Duran, Electrochemical behavior of SiO_2 sol–gel coatings on stainless steels, J. Sol–Gel Sci. Technol. 4 (1995) 239–244.
[5] P. Galliano, J.J. de Damborenea, M.J. Pascual, A. Duran, Sol–gel coatings on 316L stainless steel for clinical applications, J. Sol–Gel Sci. Technol. 13 (1998) 723–727.
[6] P. Li, K. de Groot, T. Kokubo, Bioactive $Ca_{10}(PO_4)_6(OH)_2$–TiO_2 composite coating prepared by sol–gel process, J. Sol–Gel Sci. Technol. 7 (1996) 27–34.
[7] C. Ohtsuki, T. Kokubo, T. Yamamuro, Mechanism of apatite formation on CaO–SiO_2–P_2O_5 glasses in a simulated body fluid, J. Non-Cryst. Solids 143 (1992) 84–92.
[8] O. Peitl, E. Zanotto, L. Hench, Highly bioactive P_2O_5–Na_2O–CaO–SiO_2 glass–ceramics, J. Non-Cryst. Solids 292 (2001) 115–126.
[9] X. Liu, C. Ding, P.K. Chu, Mechanism of apatite formation on wollastonite coatings in simulated body fluids, Biomaterials 25 (10) (2004) 1755–1761.
[10] T. Kokubo, H. Kim, M. Kawashita, Novel bioactive materials with different mechanical properties, Biomaterials 24 (2003) 2161–2175.
[11] L.E. Amato, D.A. Lopez, P.G. Galliano, S.M. Cere, Electrochemical characterization of sol–gel hybrid coatings in cobalt-based alloys for orthopaedic implants, Mater. Lett. 59 (16) (2005) 2026–2031.

[12] J. Ballarre, J.C. Orellano, C. Bordenave, P. Galliano, S. Ceré, In vivo and in vitro evaluation of vitreous coatings on cobalt based alloys for prothetics devices, J. Non-Cryst. Solids 304 (5) (2002) 278–285.
[13] S. Pellice, P. Galliano, Y. Castro, A. Durán, Hybrid sol–gel coatings produced from TEOS and gamma-MPS, J. Sol–Gel Sci. Technol. 28 (2003) 81–86.
[14] J. Ballarre, D.A. López, A.L. Cavalieri, Nanoindentation of hybrid silica coatings on surgical grade stainless steel, Thin Solid Films 516 (2008) 1082–1087.
[15] R. Prikryl, V. Cech, L. Zajickova, J. Vanek, S. Behzadi, F.R. Jones, Mechanical and optical properties of plasma-polymerized vinyltriethoxysilane, Surf. Coat. Technol. 200 (1–4) (2005) 468–471.
[16] J. Malzbender, G. de With, J.M.J. den Toonder, Elastic modulus, indentation pressure and fracture toughness of hybrid coatings on glass, Thin Solid Films 366 (1–2) (2000) 139–149.
[17] V.A. Soloukhin, W. Posthumus, J.C.M. Brokken-Zijp, J. Loos, G. de With, Mechanical properties of silica-(meth)acrylate hybrid coatings on polycarbonate substrate, Polymer 43 (23) (2002) 6169–6181.
[18] G. Wei, B. Bhushan, S. Joshua Jacobs, Nanomechanical characterization of multilayered thin film structures for digital micromirror devices, Ultramicroscopy 100 (3–4) (2004) 375–389.
[19] S. Simunkova, O. Blahova, I. Stepanek, Mechanical properties of thin film-substrate systems, J. Mater. Process. Technol. 133 (1–2) (2003) 189–194.
[20] L.-Y. Huang, J.-W. Zhao, K.-W. Xu, J. Lu, A new method for evaluating the scratch resistance of diamond-like carbon films by the nano-scratch technique, Diam. Relat. Mater. 11 (7) (2002) 1454–1459.
[21] X. Li, M. Huang, M. Curry, S. Street, M. Weaver, Nanoscratch behavior of dendrimer-mediated Ti thin films, Tribol. Lett. 19 (4) (2005) 273–280.
[22] T.W. Scharf, J.A. Barnard, Nanotribology of ultrathin a:SiC/SiC–N overcoats using a depth sensing nanoindentation multiple sliding technique, Thin Solid Films 308–309 (1997) 340–344.
[23] C.M. Lepienski, C.E. Foerster, in: H.S. Nalwa (Ed.), Review Chapter: Nanomechanical Properties by Nanoindentation, American Scientific Publishers, Stevenson Ranch, USA, 2004.
[24] J. Malzbender, J. den Toonder, A. Balkenende, G. de With, Measuring mechanical properties of coatings: a methodology applied to nano-particle-filled sol–gel coatings on glass, J. Mater. Sci. Eng. R 36 (2002) 47–103.
[25] M. Bonne, B. Briscoe, C. Lawrence, S. Manimaaran, D. Parsonage, A. Allan, Nanoindentation of scratched poly(methyl methacrylate) surfaces, Tribol. Lett. 18 (2) (2005) 125–133.